Solar-Terrestrial Physics. 2023. Vol. 9. Iss. 1. P. 21–30. DOI: 10.12737/stp-91202303. © 2023
T.D. Borisova, N.F. Blagoveshchenskaya, A.S. Kalishin. Published by INFRA-M Academic Publishing House

UDC 533.951, 537.868
DOI: 10.12737/stp-91202303

Received November 22, 2022
Accepted February 21, 2023

FEATURES OF ARTIFICIAL IONOSPHERE TURBULENCE INDUCED BY THE O- AND X-MODE HF HEATING NEAR THE F2-LAYER CRITICAL FREQUENCY

T.D. Borisova
Arctic and Antarctic Research Institute,
St. Petersburg, Russia, borisova@aari.ru

A.S. Kalishin
Arctic and Antarctic Research Institute,
St. Petersburg, Russia, askalishin@aari.ru

N.F. Blagoveshchenskaya
Arctic and Antarctic Research Institute,
St. Petersburg, Russia, nataly@aari.ru

Abstract. We present experimental results from the studies of large-scale inhomogeneities along the external magnetic field with increased electron density, electron temperature, and excitation of elongated plasma waves (Langmuir and ion-acoustic), induced by the ordinary (O-mode) and extraordinary (X-mode) HF heating near the F2-layer critical frequency, in the high-latitude ionospheric F-region. The experiments have been carried out at the EISCAT/Heating facility (Tromsø, Norway). Powerful HF radio waves radiated toward the magnetic zenith through a step change in the effective radiated power at frequencies f_H near and below the F2-layer critical frequency f_oF2. The EISCAT incoherent scatter radar (930 MHz), co-located with the EISCAT/Heating facility, was utilized for diagnostics of ionospheric modification effects. We calculated the electric field of a powerful HF radio wave near the reflection altitude, taking into account the non-deflective absorption along the propagation path. We determined the conditions for electric field generation and its threshold (minimum) values required for electron density enhancements in a wide altitude range, excitation of Langmuir and ion-acoustic plasma waves under f_H~f_oF2 and f_H<f_oF2. The possible generation mechanisms for the electron density enhancements above the reflection altitude of the powerful HF radio wave of O- and X-polarization are discussed.

Keywords: high-latitude ionosphere, F-region, powerful HF radio wave, electric field, electron density enhancement, Langmuir wave, ion-acoustic wave, incoherent scatter radar, EISCAT.

INTRODUCTION

The nonlinear interaction between powerful HF radio waves and ionospheric plasma are currently being extensively studied. Modifications of the upper (F-region) ionosphere by powerful HF radio waves of ordinary (O-mode) or extraordinary (X-mode) polarization leads to generation of artificial ionospheric irregularities, excitation of plasma waves, stimulated electromagnetic emission (broadband, narrowband), optical radiation, etc. [Gurevich, 2007; Frolov et al., 2007; Blagoveshchenskaya, 2020; Robinson, 1989]. Effectiveness of heater radiation effect on the ionospheric F-region depends on the latitude of its location, effective radiated power (ERP), direction of radiation relative to the orientation of the magnetic field, frequency of the pump wave f_H and its polarization, background heliophysical conditions.

According to theoretical concepts, only O-mode powerful HF radio waves with a frequency below the F2-layer critical frequency (f_H<f_oF2) can excite electrostatic plasma waves (Langmuir and upper hybrid) in the ionospheric F-region since X-mode radio waves do not reach resonant altitudes in the ionosphere [Gurevich, 2007; Stubbe, Kopka, 1983; Robinson, 1989]. Near the reflection altitude of a powerful HF radio wave, parametric decay instabilities — periodic two-stream and oscillating two-stream, which can be directly identified in spectra of a scattered signal, recorded by an incoherent scatter (IS) radar, as HF-induced plasma lines (HFPL) and HF-enhanced ion lines (HFIL) — are excited in the ionosphere [Kuo, 2001; Kuo, Lee, 2005; Stubbe, 1996; DuBois et al., 1990; Djuth, DuBois, 2015]. The appearance of HFIL and HFPL in the spectra of the scattered signal detected by the IS radar is direct evidence of the excitation of elongated plasma waves (Langmuir and ion-acoustic) and hence of the development of parametric decay two-stream instabilities.

When heated by O-mode waves (O-mode heating), HFPL and HFIL are excited during the initial time period (<200 ms) when the heater is turned on (“overshoot” effect), threshold powers of their excitation at the EISCAT/Heating facility are ~25–40 MW [Stubbe, 1996]. At *ERP*<200 MW, the excitation of parametric two-stream instabilities is suppressed by the subsequent development of a thermal parametric (resonant) instability [Vas'kov, Gurevich, 1979; Grach et al., 1977; Stubbe, 1996] responsible for the generation of small-scale field-aligned artificial ionospheric irregularities. At *ERP*>200 MW, the excitation of HFIL and HFPL, which exist simultaneously with small-scale artificial ionospheric irregularities, can be restarted [Borisova et al., 2017; Blagoveshchenskaya et al., 2020].

An X-mode powerful HF radio wave in the ionosphere is reflected at the altitude where the local plasma frequency is defined as $f_{pe}^2 = f_H(f_H - f_{ce})$, where f_{ce} is the electron gyrofrequency, i.e. below altitudes of excitation of electrostatic plasma waves. Thus, X-mode powerful HF radio waves should not generate such waves and, accordingly, cause artificial plasma turbulence and related phenomena since X-mode waves do not reach heights of ionospheric resonances [Stubbe, Kopka, 1983; Robinson, 1989; Gurevich, 2007]. The results of numerous experiments carried out at the EISCAT/Heating facility in the mode of radiation of X-mode HF radio waves (X-mode HF heating) into the high-latitude ionospheric F-region toward the magnetic zenith have demonstrated that various phenomena can occur in F-region plasma. At the same time, the X-mode pump wave induced effects can be much stronger than those produced by O-mode HF heating [Blagoveshchenskaya et al., 2018, 2019; Blagoveshchenskaya, 2020; Blagoveshchenskaya et al., 2022]. Let us mention such phenomena as generation of artificial ionospheric irregularities, intense Langmuir and HF-enhanced ion lines, strong increases in electron density in a wide range of altitudes (200–450 km above the F2-layer maximum). At X-mode heating at high frequencies (f_H=5.4–8 MHz) at *ERP*>250 MW, strong increases in N_e were recorded at pump wave frequencies both below and above the F2-layer critical frequency [Blagoveshchenskaya et al., 2022]. According to the studies carried out at the high-latitude EISCAT/Heating facility [Blagoveshchenskaya et al., 2022], the N_e increases may run to 50–70 % relative to N_{e0}, forming channels of increased electron density (ducts) along the magnetic field, which occurs with relatively small increases in electron temperature T_e (~20–30 % when heated at $f_H \leq f_o$F2 and to 40–50 % when heated at $f_H > f_o$F2) due to ohmic electron heating. N_e began to increase after the heater was switched on and reached maximum values in ~30–50 s. After the heater was switched off, N_e returned to the background level in 2–5 min.

Unlike X-mode heating at which the N_e increase in a wide range of heights is a typical phenomenon, at O-mode heating N_e can increase in the F-region to 450–550 km only under specific conditions. As observed by the EISCAT IS radar, under these conditions the pump wave frequency should be near the F2-layer critical frequency, $f_H \sim f_o$ F2, and near or above the electron gyroharmonic frequency, $f_H \geq nf_{ce}$, where n is the harmonic number [Borisova et al., 2015]. HAARP (High-frequency Active Auroral Research Program) experiments with the aid of the DEMETER and DMSP satellites have found channels of increased-density plasma (atomic oxygen ions O^+ and electrons) at 670–840 km when the F-region was heated by O-mode powerful HF radio waves. The most intense ducts were at the pump wave frequencies near the F2-layer critical frequency and the second electron gyrocharmonic [Vartanyan et al., 2012; Milikh et al., 2012]. The results of the studies carried out in [Rapoport et al., 2007; Frolov et al., 2008] also with the DEMETER and DMSP satellites have demonstrated that the channels of increased-density plasma (O^+ ions and electrons) can be formed at altitudes of 660 and 840 km when the F2-region is modified by O-mode powerful HF radio waves, using the mid-latitude heating facility Sura.

The purpose of this work is to determine excitation thresholds, i.e. minimum values of powerful HF radio wave electric field strength required to form channels of increased electron density and to excite Langmuir and ion-acoustic waves at O- and X-mode heating of the F-region. The research is based on experimental data from the EISCAT/Heating facility and on the results of numerical calculations of the pump wave electric field strength E_{ion} in the ionosphere, taking into account losses of the powerful wave during its propagation in underlying layers.

1. GENERAL CHARACTERISTICS OF THE EXPERIMENTS

Experiments with a stepwise change in the effective radiated power of O- or X-mode powerful HF radio waves were carried out at the high-latitude heating facility EISCAT/Heating (Tromsø, Norway) [Rietveld et al., 2016] on February 26, 2013 from 12:30 to 13:30 UT and on October 20, 2012 from 13:30 to 14:30 UT. On February 26, 2013, a powerful HF radio wave was emitted at a frequency f_H=7.1 MHz, close to the F2-layer critical frequency (f_H/f_oF2~0.99–1.05, hereinafter referred to as f_H/f_oF2~1), which was higher than the fifth electron gyroharmonic frequency by 0.26 MHz. On October 20, 2012, the radiation was emitted at f_H=7.953 MHz lying below f_oF2 (f_H/f_oF2~0.89–0.94) and below (by 0.187 MHz) the frequency of the sixth electron gyroharmonic. Both experiments used phased array No. 1 with a bandwidth ~5°–6° at a level of –3 dB, oriented toward the magnetic zenith (the HF heater beam was tilted to the south from the vertical direction by 12°, the azimuth was 185°). The radiation was emitted for 10 min with a stepwise change in *ERP* every minute, followed by a 5 min pause. Polarization of the powerful HF radio wave changed in each cycle.

On February 26, 2013 from 12:30 to 13:30 UT, the effective radiated power of the EISCAT/Heating facility varied in the heating cycle from 80 to 690 MW. The calculated *ERP* values were approximately equal for each heating cycle (of the four presented) and amounted, with a per-minute stepwise change (with a 1 s pause between the steps), to 12, 27, 55, 77, 100, 100, 77, 55, 27, and 12 % of ERP_{max}~690 MW. The experiment was conducted during the daytime under moderate solar activity (Wolf number W=59 [https://spaceweather.com]), under quiet geomagnetic conditions (K_p=2– and A_p=6 [https://wdc.kugi.kyoto-u.ac.jp]).

On October 20, 2012 from 13:30 to 14:30 UT, *ERP* varied in a stepwise manner in the sequence of 10, 30, 50, 70, 100, 100, 70, 50, 30, 10 % from ERP_{max}≈585 MW.

Diagnostics of phenomena in the high-latitude ionospheric F-region during the experiments was carried out by the IS radar (Tromsø) at a frequency of 930 MHz belonging to EISCAT (European Incoherent Scatter)

Scientific Association [Rishbeth, van Eyken, 1993], which is co-located with the heater. The spatial scale (wavelength) of scattering turbulence for the EISCAT IS radar l=0.16 m ($l=c/2\ f_{\rm rad}$, where c is the speed of light). With the EISCAT radar, the following parameters of ionospheric plasma were determined: electron density $N_{\rm e}$ and temperature $T_{\rm e}$, intensity of heating induced spectral lines (spectral maxima of Langmuir $S_{\rm PL}$ and ion-acoustic $S_{\rm IL}$ waves), as well as the scattered radar signal power (raw electron density values) $N_{\rm raw}$. During the experiments, the IS radar operated in an altitude range from 90 to 680 km with a height resolution of 3 km and a time resolution of 5 s. The radar beam was directed toward the powerful HF radio wave and oriented along the geomagnetic field.

Ionospheric conditions and F2-layer critical frequencies were monitored using a vertical sounding ionosonde located in Tromsø.

2. OBSERVATIONAL RESULTS

In this section, we use EISCAT IS radar observations (930 MHz) to examine the $N_{\rm e}$ and $T_{\rm e}$ behavior, raw values of electron density $N_{\rm raw}$ and HFPL intensity $S_{\rm PL}$ with a stepwise change in the effective radiated power of the EISCAT/Heating facility during the experiments on February 26, 2013 and October 20, 2012.

From the $N_{\rm raw}$ data, using the Grand Unified Incoherent Scatter Design and Analysis Package system (GUISDAP) [Lehtinen, Huuskonen, 1996], we calculated $N_{\rm e}$ and $T_{\rm e}$. Distributions of $N_{\rm e}$ and $T_{\rm e}$ as a function of time t (UT) and height h were obtained with a time integration step of 30 s and a variable height step. When elongated plasma waves (ion-acoustic and Langmuir) are excited in the ionosphere, coherent scattering of radar signal occurs. The incoherent scattering theory, embedded in GUISDAP, does not allow us to reliably identify the ionospheric parameters at the altitudes of excitation of elongated plasma waves; therefore, we considered only reliable data in the analysis, which are programmatically controlled by the level of the parameter Residual<2.1 [Lehtinen, Huuskonen, 1996]. GUISDAP was also used to estimate the plasma line intensities $S_{\rm PL}$ measured near the pump wave frequency $f_{\rm H}$ in an altitude range 128÷302 km. Note that during the experiments, the EISCAT radar in the high-frequency measurement channel recorded plasma waves shifted down in frequency relative to the radar frequency (the frequency changes are marked with minus in Figures). Graphical representation of the integration results was performed in MatLab or GUISDAP.

Figures 1, 2 present the results of processing of the IS radar's data obtained during the heating experiments on February 26, 2013 from 12:30 to 13:30 UT and on October 20, 2012 from 13:30 to 14:30 UT respectively, with a stepwise change in the effective radiated power. Panels *a*, *b*, and *c* in Figures 1 and 2 characterize altitude-time distributions of $N_{\rm e}$, $T_{\rm e}$, and $N_{\rm raw}$ describing the intensity of HF-enhanced ion-acoustic waves. Panels *d* show spectrograms of $S_{\rm PL}$ (frequency-time distributions) of HF-induced plasma lines, measured near the pump wave frequency $f_{\rm H}$ from –5.5 to –8.1 MHz on February 26, 2013 and from –7.25 to –9.2 MHz on October 20, 2012 respectively. Time variations in $N_{\rm e}$ and $T_{\rm e}$ at fixed heights are depicted in panels *e* and *f*, and panels *g* illustrate the behavior of critical frequencies of the regular F2 layer ($f_{\rm o}$F2) according to the data from the Tromsø vertical sounding station. Variations in the effective radiated power (*ERP*) of the EISCAT/Heating facility and the calculated strength of the pump wave electric field ($E_{\rm ion}$) in the ionosphere are marked in panels *h* with black and red colors respectively. The method of calculating $E_{\rm ion}$ is presented in Section 3.

Panels *a*, *e* in Figure 1 clearly demonstrate that on October 26, 2013 under conditions when the pump wave frequency $f_{\rm H}$=7.1 MHz was close to the F2-layer critical frequency and exceeded (by 0.26 MHz) the frequency of the fifth electron gyroharmonic, in all the four cycles at both X- and O-mode HF heating an increase was observed in $N_{\rm e}$ at altitudes above the reflection altitude of the powerful HF radio wave (up to ~500 km). The results of determination of $N_{\rm e}$ at fixed altitudes at O-mode HF heating suggest that the electron density increase relative to the background level $N_{\rm e0}$ was $\Delta N_{\rm e}$~21–42 % and in the cycle at 12:31–12:41 UT began when *ERP*=186 MW; and in the cycle at 13:01–13.11 UT, when *ERP*=380 MW. Hereinafter, the relative electron density increase $\Delta N_{\rm e}=(N_{\rm e}-N_{\rm e0})/N_{\rm e0}$. At X-mode HF heating, $\Delta N_{\rm e}$~45–72 %. $N_{\rm e}$ started to increase at *ERP*=186 MW in the cycle 12:46–12:56 UT and at *ERP*=83 MW in the cycle 13:16–13:26 UT. $\Delta N_{\rm e}$ increased with altitude. After the heater was switched off, at X-mode HF heating $N_{\rm e}$ remained increased for 1–2 min.

The electron density behavior on October 20, 2012 when heated at $f_{\rm H}$=7.953 MHz, which was lower than both the F2-layer critical frequency and the frequency of the sixth electron gyroharmonic (by 0.187 MHz), is illustrated in Figure 2, *a*, *e*. From the data it is clear that unlike the February 26, 2013 event there was no $N_{\rm e}$ enhancement effect during the O-mode HF heating cycles (13:31–13:41 UT and 14:01–14:11 UT). At X-mode HF heating (cycles 13:46–13:56 and 14:16–14:26 UT), as in the experiment on February 26, 2013, strong increases in $N_{\rm e}$ were detected in a wide range of altitudes, from 250–280 km, which is higher than the reflection altitude of the powerful HF radio wave, up to 600 km. The relative electron density increase was ~48–82 % and began at *ERP*=59 MW.

The $T_{\rm e}$ behavior during the experiments on February 26, 2013 and October 20, 2012 was similar (see Figure 1, *b*, *f* and Figure 2, *b*, *f*). At O-mode HF heating, strong increases in electron temperature occurred from altitudes close to the reflection and upper hybrid resonance altitudes. Then, the regions of increased $T_{\rm e}$ propagated along the magnetic field to the heights of the upper ionosphere due to the longitudinal transfer of thermal conductivity in magnetized plasma [Gurevich, 2007]. The electron temperature during the O-mode HF heating cycles in the F-region was as high as 2500–3500 K, exceeding background $T_{\rm e}$ by 1000–1500 K.

Increases in $T_{\rm e}$ during the X-mode HF heating cycles were significantly lower than those at O-mode HF heating and did not exceed 500–700 K relative to the background level. They occurred in a relatively narrow range of altitudes near the reflection altitude of the powerful HF

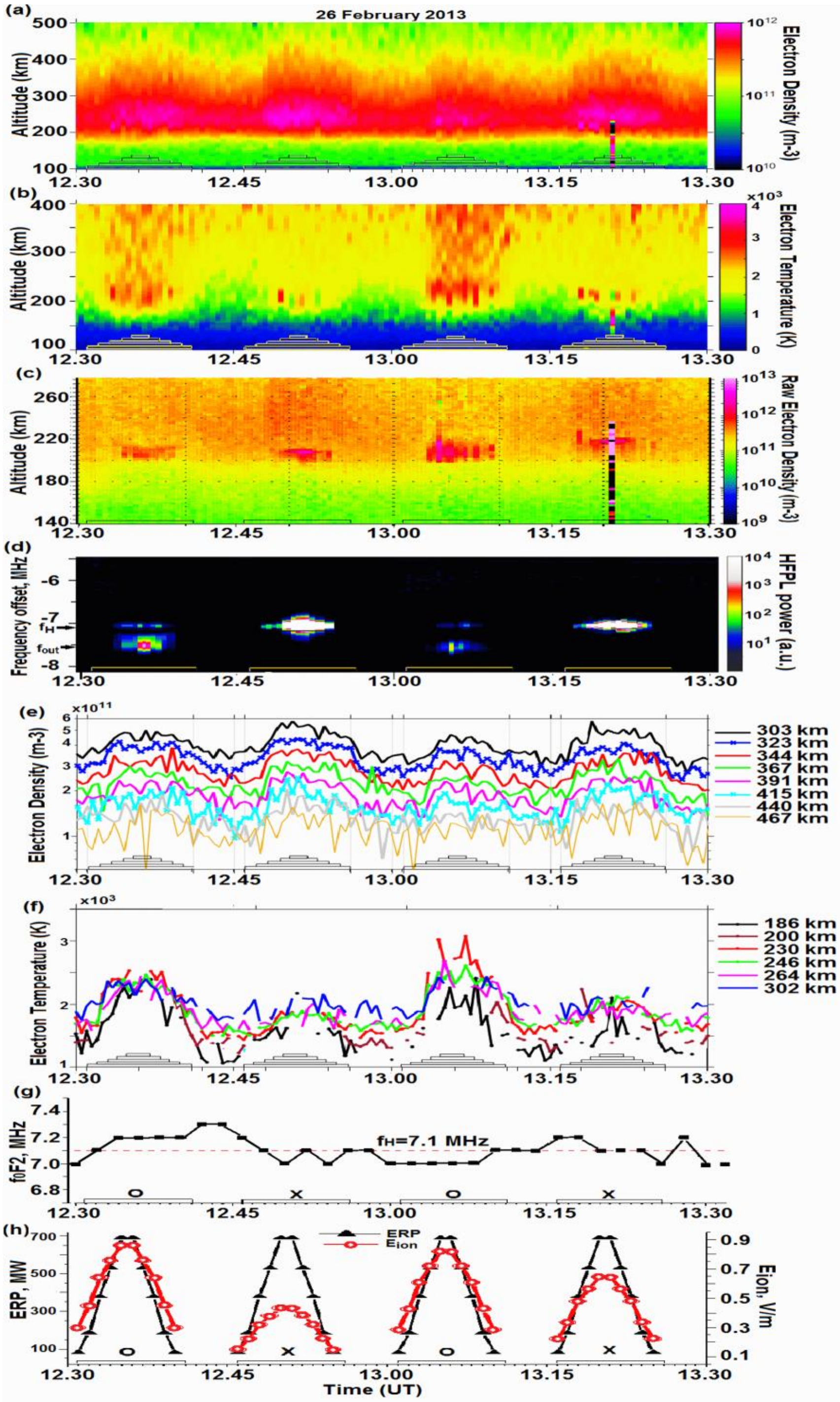

Figure 1. Altitude-time distributions of N_e, T_e, and N_{raw} (*a, b,c*); S_{PL} spectrogram (*d*); time variations in N_e and T_e at fixed ionospheric heights (*e,f*) according to EISCAT IS radar data obtained on February 26, 2013; variations in f_oF2 (*g*), as well as *ERP* (black) and the pump wave electric field E_{ion} level calculated at ionospheric heights (red) (*h*). The O/X-mode HF radio wave radiated toward the magnetic zenith at f_H=7.1 MHz with a stepwise change in *ERP* (80–680 MW). Heating cycles are plotted along the time axes

radio wave due to ohmic electron heating. Note that at both O- and X-mode HF heating, T_e increased (decreased) as the effective radiated power increased (decreased).

The altitude-time distributions of N_{raw} (see Figure 1, *b* and Figure 2, *c*), characterizing the HFIL intensity S_{IL} demonstrate that N_{raw} enhances by one or two orders of magnitude relative to the background during both O- and X-mode HF heating cycles at altitudes near the reflection altitude of the powerful HF radio wave. Simultaneously with the HFIL excitation, HFPL were excited. From the spectrograms, given in Figure 1, *d* and Figure 2, *d*, it follows that during the heating cycles HFPL formed regions of increased S_{PL} near f_H=7.1 MHz on February 26, 2013 and f_H=7.953 MHz on October 20, 2012 respectively. The plasma line intensity at X-mode HF heating significantly exceeded S_{PL} at O-mode HF heating. Note that during the February 26, 2013 O-mode HF heating cycles performed under special conditions (f_H/f_oF2~1 and

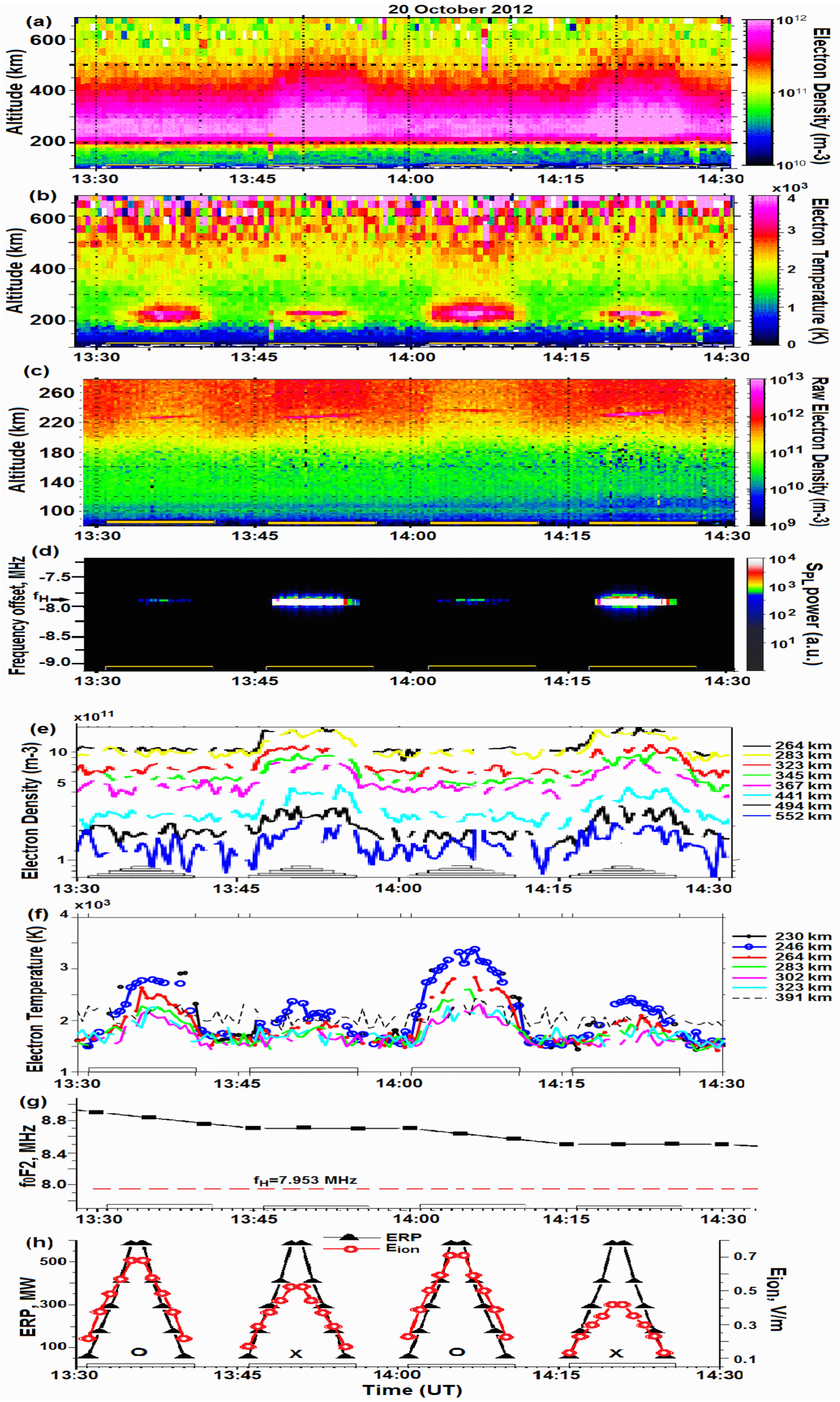

Figure 2. Altitude-time distributions of N_e, T_e, and N_{raw} (*a*, *b*, *c*); S_{PL} spectrogram (*d*); time variations in N_e and T_e at fixed ionospheric heights *h* (*e*, *f*) according to the EISCAT IS radar data obtained on October 20, 2012; variations in f_oF2 (*g*), as well as *ERP* (black) and the the pump wave electric field level E_{ion} calculated at ionospheric heights (red) (*h*). The O/X-mode HF radio wave radiated toward the magnetic zenith at f_H=7.953 MHz with a stepwise change in *ERP* (56–560 MW). Heating cycles are plotted along the time axes

f_H>5 f_{ce} at 0.26 MHz), there were regions of increased S_{PL} not only at f_H=7.1 MHz, but also at f_{out} shifted from f_H upward by ~0.40 MHz (f_{out} is plotted along the Y-axis). On October 20, 2012, no additional regions of increased S_{PL} were observed at frequencies shifted relative to f_H. Plasma lines at frequencies shifted relative to f_H at O-mode HF heating were also excited in other experiments at the EISCAT/Heating facility under conditions of proximity of the pump wave frequency to the critical F2-layer frequency and electron gyrofrequency harmonics; the excitation was attributed to dispersion properties of the Langmuir wave in a plasma with a finite electron temperature [Borisova et al., 2018; Isham et al., 1990; DuBois et al., 1990].

3. CALCULATION OF THE POWERFUL HF RADIO WAVE ELECTRIC FIELD IN THE IONOSPHERE E_{ION}

The powerful HF radio wave electric field strength of the EISCAT/Heating facility in free space is defined by the expression [Robinson, 1989]

$$E_{\rm ion}\left[\frac{V}{m}\right]=\frac{0.25\sqrt{ERP[\rm kW]}}{h[\rm km]}. \quad (1)$$

Radio wave propagation in the ionosphere occurs with the loss of part of its energy, which is generally converted into the thermal energy. These losses result in damping, i.e. a decrease in the wave field amplitude, and Expression (1) takes the form

$$E_{\rm ion}\left[\frac{V}{m}\right]=\frac{0.25\sqrt{ERP[\rm kW]}}{h[\rm km]}{\rm e}^{-A}, \quad (2)$$

where h is the current height in a disturbed region at which the wave field is calculated; A indicates the losses of radio wave intensity in dB along the propagation path s, which are calculated as [Zawdie et al., 2017]

$$A=-8.68\int\kappa ds. \quad (3)$$

In (3), ds is the distance along the propagation path; κ is the imaginary part of the wave vector **k**: $\mathbf{k}=\omega\cdot n/s$, where $\omega=2\pi f$, f is the radio signal frequency; $n=(\mu+i\chi)$ is the complex refractive index; μ is the real part of the refractive index; χ is the imaginary part of the refractive index; c is the speed of light. For κ we use the approximate expression

$$\kappa=\frac{e^2}{2\varepsilon_0 m_e c}\frac{1}{\mu}\frac{N_e\nu_e}{\nu_e^2+(\omega\pm\omega_{ce}\cos\theta)^2}, \quad (4)$$

where e, m_e is the electron charge and mass; ε_0 is the permittivity of free space; ν_e is the electron collision frequency; $\omega_{ce}=2\pi f_{ce}$; f_{ce} is the electron gyrofrequency; θ is the angle between the wave propagation direction (**k**) and the geomagnetic field. Plus/minus marks ordinary (O-mode) and extraordinary (X-mode) wave polarization respectively.

Numerical estimates of the powerful HF radio wave electric field at reflection altitudes with damping along the wave propagation path in the D, E, and F layers of the ionosphere were carried out in the geometrical optics approximation for the stratified ionosphere and implemented in MatLab. Since we deal with pump wave propagation to the reflection altitude or to the F2-layer maximum, we simplify the trajectory calculations, using Snell's law and the Breit—Tuve theorem [Davis, 1973]. The refractive index is calculated taking into account the magnetic field effect and the electron collision frequency [Ginzburg, 1967]. Zawdie et al. [2017] have demonstrated that any method of determining radio beam paths can be exploited to calculate ionospheric absorption if the electron collision frequencies ν_e are correctly applied. When calculating HF radio wave damping, we should consider variations in frequencies of collisions of electrons with ions ν_{ei} and neutral molecules ν_{en} depending on local time, season, latitude, and solar cycle (excluding collisions between electrons). These changes in absorption calculations lead to ~30 % differences in the total ionospheric attenuation.

The electron collision frequency $\nu=\nu_{ei}+\nu_{en}$. Variations in ν_{ei} were found from [Ginzburg, 1967]

$$\nu_{ei}=N_e\cdot10^{-6}\left[59+4.18\lg\left(\frac{T_e^3}{N_e}\right)\right]T_e^{-3/2}. \quad (5)$$

The ν_{en} values were calculated for three main atmospheric composition components (molecular nitrogen (N_2), molecular and atomic oxygen (O_2 and O)) from the formulas [Schunk, Nagy, 2000]:

$$\begin{aligned}\nu_{en}&=\nu_{eN_2}+\nu_{eO_2}+\nu_{eO},\\ \nu_{eN_2}&=2.33\cdot10^{-11}N_{N_2}\left(1-1.21\cdot10^{-4}T_e\right)T_e,\\ \nu_{eO_2}&=1.82\cdot10^{-11}N_{O_2}\left(1+0.036\sqrt{T_e}\right)\sqrt{T_e},\\ \nu_{eO}&=8.9\cdot10^{-11}N_{O}\left(1+5.7\cdot10^{-4}T_e\right)\sqrt{T_e}.\end{aligned} \quad (6)$$

When calculating the trajectories of powerful HF radio wave propagation and absorption, the current parameters of $N_e(h)$ and $T_e(h)$ vertical profiles for each heating cycle were determined from the IS radar's data (height resolution of 3 km). The electron collision frequencies $\nu_e(h)$ were calculated in terms of (5), (6) whose input parameters were the current data obtained from the IS radar and calculated using the MSIS model [https://ccmc.gsfc.nasa.gov/modelweb/models/msis_vitmo.php]. The powerful HF radio wave electric field E_{ion} at ionospheric heights was calculated taking into account the per-minute changes in *ERP* of the EISCAT/Heating facility.

Table presents the results of numerical estimates of the powerful HF radio wave absorption A (in dB), experimental *ERP* (in MW), at which the N_e increases and the plasma and the ion line excitation begin/cease, for the experimental conditions on February 26, 2013 and October 20, 2012 for each O- and X-mode HF heating cycle. Columns 4–6 also list values of powerful HF radio wave electric fields E_{ionNe}, E_{ionPL}, and E_{ionIL} (in V/m), calculated in view of the non-deflective absorption in the ionosphere, at which the N_e increase and the excitation of plasma and ion lines begin/cease. Column 4 additionally shows the ranges of changes in the relative electron density increases ΔN_e (in %) at 250–600 km.

4. DISCUSSION

The analysis of the data given in Table and Figures 1 and 2 suggests that during all X-mode HF heating cycles both on February 26, 2013 (f_H/f_oF2~1 and $f_H>5f_{ce}$ by 0.26 MHz) and on October 20, 2012 ($f_H/f_oF2<1$ and $f_H<6f_{ce}$ by 0.187 MHz) at ~300–600 km there were strong increases in the electron density: ΔN_e=45–82 %. Note that the electron density increase in the wide range of altitudes is a typical phenomenon for X-mode HF heating, observed in all our previous experiments with the high-latitude HF heater EISCAT/Heating (see, e.g., [Blagoveshchenskaya, 2020;

Blagoveshchenskaya et al., 2022]). The minimum (threshold) values of electric fields, calculated taking into account powerful HF radio wave damping during its propagation to ionospheric heights, in the ionosphere at X-mode HF heating, at which N_e began to increase, E_{ionNe}=0.13–0.22 V/m, which is lower than the excitation thresholds of Langmuir (E_{ionPL}=0.22–0.34 V/m) and ion-acoustic (E_{ionIL}=0.29–0.34 V/m) plasma waves (see Table). With a decrease in *ERP* in the second half of the X-mode HF heating cycles, the N_e enhancement effect disappeared later than the excitation of Langmuir and ion-acoustic plasma waves ceased. Thus, N_e began to increase before the excitation of plasma waves and stopped to increase after their excitation ceased, i.e. $E_{ionNe}<E_{ionPL}$ and $E_{ionNe}<E_{ionIL}$.

No increase in N_e generally occurs at O-mode HF heating, yet under special heating conditions ($f_H/f_oF2{\sim}1$ and $f_H{\geq}nf_{ce}$) the electron density increased in the high-latitude ionospheric F-region up to 450–550 km [Borisova et al., 2015]. Such conditions were implemented in the experiment on February 26, 2013, when the N_e enhancement effect was observed during O-mode HF heating cycles. When comparing the N_e enhancement effects occurring at O- and X-mode HF heating, the following differences have been revealed. Firstly, at O-mode HF heating, the relative electron density increases ΔN_e=21–42 % were lower than at X-mode HF heating, and their excitation thresholds E_{ionNe}=0.45–0.60 V/m exceeded the thresholds E_{ionNe} at X-mode HF heating. Secondly, an increase in N_e at O-mode HF heating occurred only in the presence of Langmuir waves, i.e. at $E_{ionNe}{\geq}E_{ionPL}$. At X-mode HF heating, the N_e increases do not depend on the behavior of Langmuir waves.

Figure 3 depicts vertical profiles of $N_e(h)$ in the height range 250–500 km for February 26, 2013 at O- (*a*, *a1*) and X-mode (*b*, *b1*) HF heating. Results of $N_e(h)$ measurements on October 20, 2012 are presented in Figure 3, *c*, *c1* for X-mode HF heating cycles. The data in Figure 3 clearly demonstrates an increase in N_e at heights above the F2-layer maximum. Discontinuities in the presented $N_e(h)$ profiles are attributed to high values of the parameter Residual when it is impossible to reliably determine N_e values.

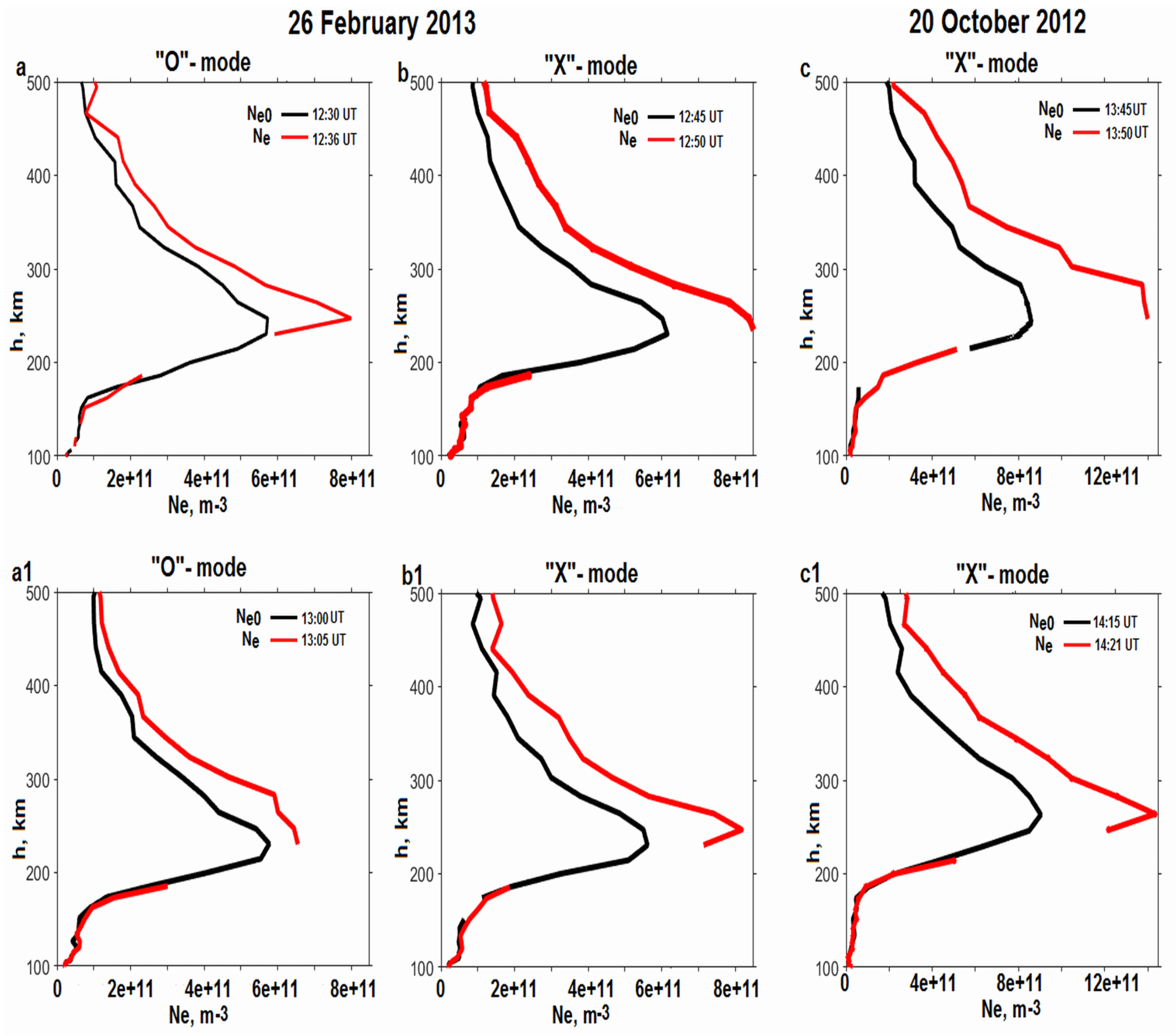

Figure 3. Electron density profiles as a function of height of the high-latitude ionosphere as derived from EISCAT radar data before the heating cycles (N_{e0}, black) and during the heating periods with 100 % *ERP* (N_e, red): February 26, 2013, $f_H/f_oF2{\sim}1$ for O-mode HF heating cycles 12:31–12:41 UT (*a*) and 13:01–13:11 UT (*a1*) and X-mode HF heating cycles 12:46–12:56 UT (*b*) and 13:16–13:26 UT(*b1*); October 20, 2012, $f_H/f_oF2<1$ for X-mode HF heating cycles 13:46–13:56 UT (*c*) and 14:16–14:26 UT (*c1*) (no N_e increase was recorded at O-mode HF heating)

The analysis of the behavior and characteristics of channels of increased N_e suggests that the X-mode powerful HF radio wave effect on the F-region toward the magnetic zenith causes electron acceleration [Blagoveshchenskaya et al., 2022]. This is due to the fact that the direction of X-mode powerful wave electric field rotation coincides with the gyration of electrons, which can lead to their acceleration. Electron acceleration at X-mode HF heating is also confirmed by the high ratio (0.35–0.5) between emission intensities of the green (557.7 nm) atomic oxygen line and the red (630 nm) optical radiation line induced by the X-mode powerful HF radio wave [Blagoveshchenskaya et al., 2014]. According to the results obtained in [Carlson et al., 1982, 2016; Carlson, Jensen, 2014; Mishin et al., 2016], the accelerated electron flux can cause ionospheric ionization to increase. A number of papers have reported results of theoretical and experimental studies on additional ionization of the ionospheric neutral component by electrons accelerated by plasma waves when the ionosphere is heated by O-mode powerful HF radio waves [Grach, 1999; Grach et al., 2016; Carlson, Jensen, 2014; Mishin et al., 2016; Carlson et al., 2016]. These studies have shown that the additional ionization by electrons accelerated by plasma turbulence is most pronounced when heated at frequencies near or above the electron gyroharmonic frequency, $f_H \geq nf_{ce}$. At the same time, the N_e enhancement effect increases when the powerful wave frequency approaches the F2-layer critical frequency. These conditions are satisfied by the February 26, 2013 experiment when an O-mode powerful HF radio wave was emitted toward the magnetic zenith at f_H=7.1 MHz, which is close to f_oF2 and slightly exceeds the frequency of the fifth electron gyroharmonic (f_H/f_oF2~1 and f_H>5 f_{ce} by 0.26 MHz). At the same time, as follows from Table, Langmuir waves were excited at E_{ionPL}~0.43–0.45 V/m, whereas N_e began to increase at higher values of E_{ionNe}~0.45–0.60 V/m. Consequently, at O-mode HF heating the excitation of Langmuir waves (HF induced plasma lines at the pump wave frequency in the high-frequency measurement channel of the EISCAT IS radar) began earlier than the N_e increase. Thus, the N_e increase at O-mode HF heating under special conditions (f_H~f_oF2 and $f_H \geq nf_{ce}$) can be explained by the occurrence of accelerated electron fluxes caused by the excitation of Langmuir turbulence. The absence of the N_e enhancement effect during the O-mode HF heating cycles on October 20, 2012 can be explained by the fact that, on the one hand, the pump wave frequency f_H=7.953 MHz was lower than the frequency of the sixth electron gyroharmonic, and, on the other hand, f_H was at a sufficient distance away from f_oF2.

Estimated absorption *A* of the powerful HF radio wave in the ionosphere, *ERP* (in parentheses), and the lowest levels of electric fields in the ionosphere required for electron density increases (E_{ionNe}) and for Langmuir (E_{ionPL}) and ion-acoustic plasma wave (E_{ionIL}) excitation for O- and X-mode HF heating cycles on February 26, 2013 and October 20, 2012, as well as ranges of changes in relative electron density increases ΔN_e at 250–600 km. The slash separates the values at which the N_e increase and the plasma and ion line excitation begin/cease

Mode, heating cycle period, UT	f_H/f_oF 2	*A*, dB	*ERP*, MW E_{ionNe}, V/m ΔN_e, %	*ERP*, MW E_{ionPL}, V/m	*ERP*, MW E_{ionIL}, V/m
1	2	3	4	5	6
February 26, 2013					
O 12:31–12:41	0.99	1.0	(186/83) 0.45/0.3 24–42	(186/186) 0.45/0.45	(380/380) 0.64/0.64
X 12:46–12:56	1.03	7.8	(186/83) 0.22/0.15 45–63	(186/186) 0.22/0.22	(380/380) 0.32/0.32
O 13:01–13:11	1.05	1.5	(380/186) 0.6/0.43 21–38	(186/83) 0.43/0.28	(380/186) 0.6/0.43
X 13:16–13:26	0.99	3.5	(83/83) 0.22/0.22 45–72	(186/186) 0.34/0.34	(186/380) 0.34/0.48
October 20, 2012					
O 13:31–13:41	0.89	1.5	–	(410/176) 0.57/0.37	(585/585) 0.68/0.68
X 13:46–13:56	0.91	3.8	(59/59) 0.17/0.17 48–64	(176/59) 0.29/0.17	(176/176) 0.29/0.29
O 14:01–14:11	0.91	1.0	–	(176/176) 0.39/0.39	(293/293) 0.5/0.5
X 14:16–14:26	0.94	5.7	(59/59) 0.13/0.13 52–82	(176/59) 0.22/0.13	(293/293) 0.29/0.29

CONCLUSION

We have presented results of the experiments at the EISCAT/Heating facility carried out on February 26, 2013 (f_H/f_oF2~1 and f_H>5 f_{ce} by 0.26 MHz) and October 20, 2012 (f_H/f_oF2<1 and f_H<6 f_{ce} by 0.187 MHz) with variable O-/X-mode HF heating of the high-latitude ionospheric F-region toward the magnetic zenith with a stepwise change in the effective radiated power. Diagnostics of the effects caused by powerful HF radio waves was made using the incoherent scatter radar EISCAT (930 MHz), co-located with the heater. We have estimated the excitation thresholds (minimum electric field strength of powerful HF radio wave in the ionosphere) required to form channels of increased electron density and to excite Langmuir and ion-acoustic waves at O- and X-mode HF heating of the F-region. The estimates were carried out taking into account the losses of the powerful wave during its propagation in the underlying layers.

It was found that at X-mode HF heating at frequencies both near and below the F2-layer critical frequency (f_H/f_oF2~1 and f_H/f_oF2<1), the electron density increases relative to the background level amount to 45–82 % at ~300–600 km. N_e began to increase at the minimum electric field of the powerful HF radio wave E_{ionNe}=0.13–0.22 V/m, which is below the excitation thresholds of Langmuir and ion-acoustic plasma waves E_{ionPL}=0.22–0.34 and E_{ionI}=0.32–0.50 V/m respectively. Consequently, N_e began to increase before the excitation of plasma waves, i.e. $E_{ionNe}<E_{ionPL}$ and $E_{ionNe}<E_{ionIL}$

At O-mode HF heating, the N_e enhancement effect was demonstrated to occur only under special conditions (f_H/f_oF2~1 and $f_H \geq nf_{ce}$). In this case, the relative electron density increases (21–42 %) were lower than at X-mode HF heating, and the thresholds of their excitation E_{ionNe}=0.45–0.60 V/m exceeded the thresholds E_{ionNe} at X-mode HF heating. Moreover, the N_e enhancement effect at O-mode HF heating was observed only in the presence of Langmuir waves, i.e. at $E_{ionNe} \geq E_{ionPL}$. At X-mode HF heating, the N_e increases do not depend on the behavior of Langmuir waves.

We have explored possible mechanisms responsible for the electron density increases above the powerful wave reflection altitude. At X-mode HF heating toward the magnetic zenith, the agreement between the X-mode powerful wave electric field rotation and the electron gyration can cause electrons to accelerate. The accelerated electron flux leads to an increase in the electron density. At O-mode HF heating, the N_e enhancement effect can be explained by the occurrence of accelerated electron fluxes caused by the excitation of Langmuir turbulence under conditions f_H~f_oF2 and $f_H>nf_{ce}$. The N_e increase at X- and O-mode HF heating requires further study.

We acknowledge the international scientific association EISCAT, which is supported by the scientific organizations of China (CRIRP), Finland (SA), Japan (NIPR and STEL), Norway (NFR), Sweden (VR), and the UK (NERC), and M.T. Rietveld for calculations of actual effective radiated powers of the EISCAT/Heating facility during the experiments.

We do not have any conflict of interest.

The work was financially supported by the Russian Science Foundation (Grant No. 22-17-00020), https://rscf.ru/project/22-17-00020.

REFERENCES

Blagoveshchenskaya N.F. Perturbing the high-latitude upper ionosphere (F region) with powerful HF radio waves: A 25-year collaboration with EISCAT. *URSI Radio Science Bulletin*. 2020, vol. 373, pp. 40–55. DOI: 10.23919/URSIRSB.2020.9318436.

Blagoveshchenskaya N.F., Borisova T.D., Kosch M., Sergienko T., Brändström U., Yeoman T.K., Häggström I. Optical and ionospheric phenomena at EISCAT under continuous X-mode HF pumping. *J. Geophys. Res.: Space Phys*. 2014, vol. 119, pp. 10483–10498. DOI: 10.1002/2014JA020658.

Blagoveshchenskaya N.F., Borisova T.D., Kalishin A.S., Kayatkin V.N., Yeoman T.K., Häggström I. Comparison of the effects induced by the ordinary (O-mode) and extraordinary (X-mode) polarized powerful HF radio waves in the high-latitude ionospheric F region. *Cosmic Research*. 2018, vol. 56, no. 1, pp. 11–25. DOI: 10.1134/S0010952518010045.

Blagoveshchenskaya N.F., Borisova T.D., Kalishin A.S., Schmelev Y.A., Leonenko E.E., Yeoman T.K. Characterization of artificial, small-scale, ionospheric irregularities in the high-latitude F region induced by high-power, high-frequency radio waves of extraordinary polarization. *Geomagnetism and Aeronomy*. 2019, vol. 59, no. 6, pp. 713–725. DOI: 10.1134/S00 16793219060045.

Blagoveshchenskaya N.F., Borisova T.D., Kalishin A.S., Yeoman T.K., Häggström I. Distinctive features of Langmuir and ion-acoustic turbulences induced by O- and X-mode HF pumping at EISCAT. *J. Geophys. Res.: Space Phys*. 2020, vol. 125, e2020JA028203. DOI: 10.1029/2020JA028203.

Blagoveshchenskaya N.F., Borisova T.D., Kalishin A.S., Egorov I.M., Zagorskiy G.A. Disturbances of electron density in the high latitude upper (F-region) ionosphere induced by X-mode HF pump waves from EISCAT UHF radar observations. *Arctic and Antarctic Research*. 2022, vol. 68, no. 3, pp. 248–257. DOI: 10.30758/0555-2648-2022-68-3-248-257.

Borisova T.D., Blagoveshchenskaya N.F., Kalishin A.S., Rietveld M.T., Yeoman T.K., Häggström I. Modification effects of the high-latitude ionospheric F region by high-power HF radio waves at frequencies near the fifth and sixth electron gyroharmonics. *Izvvestiya vuzov. Radiofizika*. [Radiophysics and Quantum Electronics]. 2015, vol. 58, no. 8, pp. 623–650. (In Russian).

Borisova T.D., Blagoveshchenskaya N.F., Yeoman T.K., Häggström I. Excitation of artificial ionospheric turbulences in the high-latitude ionospheric F region as a function of the EISCAT/Heating effective radiated power. *Izvvestiya vuzov. Radiofizika*. [Radiophysics and Quantum Electronics]. 2017. vol. 60, no. 4, pp. 305–325. (In Russian).

Borisova T.D., Blagoveshchenskaya N.F., Rietveld M.T., Häggström I. Outshifted plasma lines observed in heating experiments in the high-latitude ionosphere at pump frequencies near electron gyroharmonics. *Izvvestiya vuzov. Radiofizika*. [Radiophysics and Quantum Electronics]. 2018, vol. 61, no. 10, pp. 810–830. (In Russian).

Carlson H.C., Wickwar V.B., Mantas G.P. Observations of fluxes of suprathermal electrons accelerated by HF excited instabilities. *J. Atmos. Terr. Phys*. 1982, vol. 44, pp. 1089–1100.

Carlson H.C., Jensen J.B. HF accelerated electron fluxes, spectra, and ionization. *Earth, Moon, and Planets*. 2014, vol. 116, pp. 1–18. DOI: 10.1007/s11038-014-9454-6.

Carlson H.C., Djuth F.T., Zhang L.D. Creating space plasma from the ground. *J. Geophys. Res.: Space Phys*. 2016, vol. 122, pp. 978–999. DOI: 10.1002/2016JA023880.

Djuth F.T., DuBois D.F. Temporal development of HF-excited Langmuir and ion turbulence at Arecibo. *Earth Moon Planets*. 2015, vol. 116, pp. 19–53. DOI: 10.1007/s11038-015-9458-x.

Du Bois D.F., Rose H.A., Russell D. Excitation of strong Langmuir turbulence in plasmas near critical density: Application to HF heating of the ionosphere. *J. Geophys. Res*. 1990, vol. 95, pp. 21221–21272.

Davies K. *Ionospheric Radio Waves*. Moscow, Mir Publ., 1973. 504 p. (In Russian). (English edition: Davies K. *Ionospheric Radio Waves*. Blaisdell Publishing Company, 1969, 460 p.)

Frolov V.L., Bakhmet'eva N.V., Belikovich V.V., Vertogradov G.G., Vertogradov V.G., Komrakov G.P., et al. Modification of Earth's ionosphere by powerful HF radiation. *Physics-Uspekhi*. 2007, vol. 50, no. 3, p. 315. DOI: 10.1070/PU2007v050n03ABEH006282.

Frolov V.L., Rapoport V.O., Komrakov G.P., Belov A.S., Markov G.A., Parrot M., Rauch J.L., Mishin E.V. Density ducts formed by heating the Earth's ionosphere with high-power HF radio waves. *Pis'ma v Zh. `Eksper. Teoret. Fiz.* [JETP Letters]. 2008, vol. 88, iss. 12, pp. 908–913. (In Russian).

Ginzburg V.L. *The Propagation of Electromagnetic Waves in Plasma*. Moscow, Nauka Publ., 1967. 684 p. (In Russian). (English edition: Ginzburg V.L. *The Propagation of Electromagnetic Waves in Plasma*. Pergamon Press, 1970, 615 p.)

Grach S.M., Karashtin A.N., Mityakov N.A., Rapoport V.O., Trakhtengerts V.Yu. Parametric interaction between electromagnetic radiation and ionospheric plasma. *Izvestya vuzov. Radiofizika*. [Radiophysics and Quantum Electronics]. 1977, vol. 20, pp. 1827–1833. (In Russian).

Grach S.M. On kinetic effects in the ionospheric F-region modified by powerful radio waves. *Radiophysics and Quantum Electronics*. 1999, vol. 42, no. 7, pp. 572–588. DOI: 10.1007/BF02677563.

Grach S.M., Sergeev E.N., Mishin E.V., Shindin A.V. Dynamic properties of ionospheric plasma turbulence driven by high-power high-frequency radiowaves. *Physics-Uspekhi*. 2016, vol. 59, no. 11, 1091 DOI: 10.3367/UFNe.2016.07.037868.

Gurevich A.V. Nonlinear effects in the ionosphere. *Physics-Uspekhi*. 2007, vol. 50, no. 11, 1091. DOI: 10.1070/PU2007 v050n11ABEH006212.

Isham B., Kofman V., Hagfors T., Nordling J., Thidé B., LaHoz C., Stubbe P. New phenomena observed by EISCAT during an RF ionospheric modification experiment. *Radio Sci*. 1990, vol. 25, no. 3, pp. 251–262.

Kuo S.P. Cascade of the parametric decay instability in ionospheric heating experiments. *J. Geophys. Res.: Space Phys*. 2001, vol. 106, pp. 5593–5597.

Kuo S.P., Lee M.C. Cascade spectrum of HF enhanced plasma lines generated in HF heating experiments. *J. Geophys. Res*. 2005, vol. 110, iss. A1, p. A01309. DOI: 10.1029/2004JA010674.

Lehtinen M.S., Huuskonen A. General incoherent scatter analysis and GUISDAP. *J. Atmos. Terr. Phys*. 1996, vol. 58, no. 1-4, pp. 435–452.

Milikh G.M., Demekhov A., Vartanyan A., Mishin E.V., Huba J. A new model for formation of artificial ducts due to ionospheric HF-heating. *Geophys. Res. Lett*. 2012, vol. 39, no. 10. L10102. DOI: 10.1029/2012GL051718.

Mishin E., Watkins B., Lehtinen N., Eliasson B., Pedersen T., Grach S. Artificial ionospheric layers driven by high-frequency radiowaves: An assessment. *J. Geophys. Res.: Space Phys*. 2016, vol. 121, pp. 3497–3524. DOI: 10.1002/2015JA021823.

Rapoport V.O., Frolov V.L., Komrakov G.P., Markov G.A., Belov A.S., Parrot M., Rauch J.L. Some results of measuring the characteristics of electromagnetic and plasma disturbances stimulated in the outer ionosphere by high-power high-frequency radio emission from the "Sura" facility. *Radiophysics and Quantum Electronics*. 2007, vol. 50, no. 8, pp. 645–656.

Rietveld M.T., Senior A., Markkanen J., Westman A. New capabilities of the upgraded EISCAT high-power HF facility. *Radio Sci*. 2016, vol. 51, no. 9, pp. 1533–1546. DOI: 10.1002/2016RS006093.

Rishbeth H., van Eyken A.P. EISCAT — early history and the first ten years of operation. *J. Atmos. Terr. Phys*. 1993, vol. 55, no. 4-5, pp. 525–542.

Robinson T.R. The heating of the high latitude ionosphere by high power radio waves. *Phys. Rep*. 1989, vol. 179, no. 2-3, pp. 79–209.

Schunk R.W., Nagy A.F. Ionospheres: Physics, Plasma Physics, and Chemistry. Cambridge, Cambridge Univ. Press, 2000, 554 p.

Stubbe P., Kopka H. Summary of results obtained with the Tromso heating facility. *Radio Sci*. 1983, vol. 18, no. 6, pp. 831–834. DOI: 10.1029/RS018i006p00831.

Stubbe P. Review of ionospheric modification experiments in Tromsø. *J. Atmos. Terr. Phys*. 1996, vol. 58, no. 1-4, pp. 349–386.

Vartanyan A., Milikh G.M., Mishin E., Parrot M., Galkin I., Reinisch B., et al. Artificial ducts caused by HF heating of the ionosphere by HAARP. *J. Geophys. Res*. 2012, vol. 117, A10307. DOI: 10.1029/2012JA017563.

Vas'kov V.V., Gurevich A.V. Self-focusing and resonant instability in the ionospheric F region. *Teplovyye nelineinyye yavleniya v plazme* [Thermal Nonlinear Phenomena in Plasma]. Gorky, IPF AN SSSR, 1979, pp. 81–138. (In Russian).

Zawdie K.A., Drob D.P., Siskind D.E., Coker C. Calculating the absorption of HF radio waves in the ionosphere. *Radio Sci*. 2017, vol. 52, pp. 767–783. DOI: 10.1002/2017RS006256.

URL: https://spaceweather.com (accessed March 1, 2023).

URL: https://ccmc.gsfc.nasa.gov/modelweb/models/msis_vitmo.php (accessed March 1, 2023).

URL: https://wdc.kugi.kyoto-u.ac.jp (accessed March 1, 2023).

Original Russian version: Borisova T.D., Blagoveshchenskaya N.F., Kalishin A.S., published in Solnechno-zemnaya fizika. 2023. Vol. 9. Iss. 1. P. 22–33. DOI: 10.12737/szf-91202303.

How to cite this article

Borisova T.D., Blagoveshchenskaya N.F., Kalishin A.S. Features of artificial ionosphere turbulence induced by the O- and X-mode HF heating near the F2-layer critical frequency. *Solar-Terrestrial Physics*. 2023. Vol. 9. Iss. 1. P. 21–30. DOI: 10.12737/stp-91202303.